# Solid-State Diffusion Welding of Wrought AISI 304 Stainless Steel to Nimonic AP-1 Superalloy Powder by Hot Isostatic Pressing

*Dissimilar materials like stainless steels and powder metallurgy superalloys can be joined by diffusion welding using hot isostatic pressing technique*

BY M. C. SOMANI, N. C. BIRLA AND A. TEKIN

ABSTRACT. The diffusion welding characteristics of wrought AISI 304 stainless steel to a superalloy powder Nimonic AP-1 were examined in this study. After encapsulation, evacuation and degassing, the welds were hot isostatically pressed (HIPed) in two different cycles, *i.e.*, 1200°C (2192°F)/3 h/ 147 MPa and 1270°C (2318°F)/3 h/ 121 MPa. A variation in surface condition of stainless steel was also studied for its influence on properties of the joints. These diffusion-welded joints were characterized for diffusion of alloying elements, microstructural features and tensile properties.

Most specimens showed good weld strength for both the hot isostatic pressing (HIP) cycles, except specimens with sand blasted surfaces, which gave negligible ductility because of the presence of sand particles embedded on the surface. In general, the tensile properties of the diffusion welded specimens were limited by the mechanical properties of stainless steel and not the joint interface. The microstructural examination of a HIP welded joint showed a thin weld zone of 30–40 µm. While the stainless steel region of the welded specimen showed a relatively clean structure, the Nimonic AP-1 region showed precipitation of dark particles near the interface extending over 20–60 µm. Electron microprobe analysis of the diffusion welded zone revealed enrichment of titanium-rich particles along prior particle boundaries (PPBs) near the interface. Electron microprobe analysis further revealed extensive diffusion of Ni, Co and Al elements into stainless steel and that of Fe into Nimonic AP-1 superalloy indicating complex composition of the weld interlayer.

*M. C. SOMANI and N. C. BIRLA, Scientists, are with Defence Metallurgical Research Laboratory, Hyderabad, India, and A. TEKIN is with the Department of Chemical and Metallurgical Engineering, Istanbul Technical University, Istanbul, Turkey.*

## Introduction

Diffusion welding by hot isostatic pressing, commonly known as gas pressure diffusion welding, has emerged as a potential joining process for various multiphase/dissimilar materials (Refs. 1, 2). Being a solid-state joining process, diffusion welding eliminates the problems of segregation, cracking and distortion stresses generally encountered in liquid phase welding techniques. With HIP welding, it has become possible to join even brittle materials without fracturing, and composite materials with a minimum of fiber damage. Using HIP diffusion welding, even components with complex geometries and dual properties, such as turbine wheels, have been fabricated (Refs. 3, 4).

Diffusion welding of a variety of steels with dissimilar materials such as refractory metals and hard materials has been reported in literature. For example, reasonably good welds have been reported by joining stainless steel to stellite (Refs. 5, 6), low alloy steel to nickel-based superalloy (Ref. 7) and AISI 304L grade stainless steel to Ti-6Al-4V alloy (Ref. 8). The main emphasis in all these studies was to optimize the HIP welding parameters resulting in good welds with reasonable properties. In another study, clad and bimetal components based on Ni, Co and Ti-based alloys with structural or stainless steels (Ref. 9) have been reported to be successfully developed using HIP. Kratt, *et al.* (Ref. 10), studied HIP parameters for processing of bimetallic parts with corrosion-resistant coatings. In this process, the cast or forged steel parts, which act as capsules for HIP, were diffusion welded with a powder nickel-based superalloy (Ni-Al-W-Mo alloy) that has very high corrosion-resistant properties so as to produce huge bimetallic parts. They have also (Ref. 11) characterized extensively the welding area in an HIPed steel/superalloy joint. The welding strength was reported to be better than that of steel with a complex microstructure at the interface.

In our earlier investigation (Ref. 12), an attempt was made to obtain dual properties in the nickel-based superalloy IN-100 by combining cast and powder metallurgy (P/M) structures using HIP technique. The aim of the preliminary investigation was to diffusion weld wrought AISI 304 grade stainless steel to a P/M superalloy Nimonic AP-1 (trademark of Wiggin Alloys Ltd., UK) by hot isostatic pressing (HIP) technique and characterize the weld with respect to chemical composition, distribution of alloying elements across the weld region and tensile properties. The understanding of the diffusion welded interface will ultimately lead to development of bimetallic tubings and components. Since diffusion welding is a surface contact phenomenon, the effect of contact surface conditions on room temperature tensile properties was also studied.

KEY WORDS

Solid-State Diffusion
Hot Isostatic Pressing (HIP)
Diffusion Welding
Powder Metallurgy
Superalloy
Stainless Steel
Weld Interlayer/Interface
Austenite and Martensite
Martensitic Transformation

## Experimental

Commercial grade AISI 304 stainless steel in wrought form was used for diffusion welding with Nimonic AP-1 super-

alloy powder, which was obtained from Wiggin Alloys Ltd., UK. It is a γ–γ′ superalloy with a high volume content of γ′ and is a low carbon version of Astroloy (trademark of General Electric Co., USA), in which the chemistry has been modified to minimize the prior particle boundary (PPB) effects. Argon atomized powder of –100 mesh (–150 μm) was used in these experiments. The chemical compositions of the two materials are given in Table 1. The superalloy powder was examined for shape, size distribution and topographical details in an ISI-100A scanning electron microscope (SEM).

Seamless AISI 304 stainless steel tubes of 10 mm (0.39 in.) internal diameter x 2 mm (0.079 in.) wall thickness x 60 mm (2.36 in.) length were used for leaktight encapsulation of both wrought AISI 304 stainless steel and Nimonic AP-1 powder. A schematic sketch of a HIP capsule used for diffusion welding is shown in Fig. 1. While one end of the tube was sealed by welding with a stainless steel lid, the other end was welded to a mild steel evacuation tube to facilitate high temperature outgassing of the capsules. After encapsulation of AISI 304 stainless steel and Nimonic AP-1 powder, the degassing was done at 800°C (1472°F) for 12 h to a vacuum of $10^{-5}$ mm of Hg (1.33 x $10^{-3}$ Pa). Since the tensile strength of Nimonic AP-1 alloy is two to three times higher than that of AISI 304 stainless steel, the weld strength factor will be controlled by the strength of stainless steel. Therefore, two high temperatures, *i.e.*, 1200°C (2192°F) [above γ′ solvus; ≈ 1140°C (2084°F)] and 1270°C (2318°F) [above boride solvus: ≈ 1205°C (2201°F)], were selected for hot isostatic pressing so as to obtain the best diffusional effects of alloying elements at the interface. Effects of two hot isostatic pressing (HIP) cycles *i.e.*, 1200°C (2192°F)/ 3 h/147 MPa and 1270°C (2318°F)/3 h/121 MPa on diffusion welding were investigated for room temperature tensile strength and diffusion of alloying elements at the interface and into the matrix. In each case, four different surface conditions were used: 1) smooth surface finish (S μm) by mechanical polishing; 2) sand blasted surface with approximate surface roughness of 50 μm; 3) rough surface finish (≈ 100 μm) by filing; and 4) acid pickled surface to remove any oxide layer.

The diffusion welded joints were examined by optical microscopy using standard metallographic techniques. While Kallings II etching reagent was used to reveal the microstructures of the weld interface and Nimonic AP-1 superalloy, aquaregia was used to etch the microstructure of stainless steel. Since P/M superalloy Nimonic AP-1 has a complex microstructure and there are several alloying elements in the two weld materials, particularly AP-1, the welded interlayer in one of the specimens was further characterized by X-ray elemental mapping in a

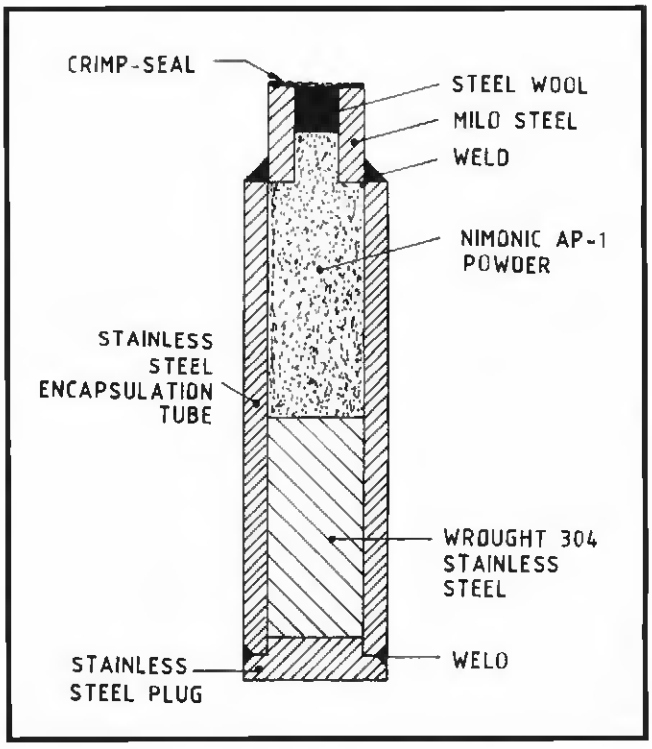


*Fig. 1 — Schematic sketch of the HIP capsule showing encapsulation of AISI 304 stainless steel (solid) and Nimonic AP-1 superalloy (powder) materials.*

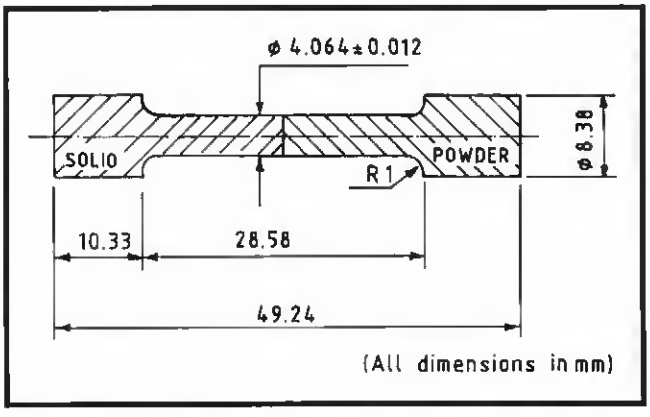


*Fig. 2 — Tensile specimen geometry for diffusion welded specimens.*

**Table 1 — Chemical Composition (Wt-%) of Diffusion Welding Materials**

| | AISI 304 Stainless Steel | | | Nimonic AP-1 Powder (–150 μm) | |
|---|---|---|---|---|---|
| Alloying Element | Specification Range | Composition | Alloying Element | Specification Range | Composition |
| C | 0.08 max | 0.07 | C | 0.02–0.04 | 0.02 |
| Cr | 17.0–20.0 | 19.3 | Cr | 14.0–16.0 | 14.8 |
| Ni | 8.0–12.0 | 9.9 | Co | 16.0–18.0 | 16.8 |
| Mn | 2.0 max | 1.4 | Mo | 4.5–5.5 | 5.0 |
| Si | 1.0 max | 0.4 | Al | 3.8–4.1 | 4.0 |
| S | 0.03 max | 0.015 | Ti | 3.3–3.6 | 3.7 |
| P | 0.045 max | 0.02 | B | 0.015–0.025 | 0.02 |
| Fe | Bal. | Bal. | Zr | — | 0.04 |
| | | | Ni | Bal. | Bal. |

Cameca Electron Probe Microanalyzer (EPMA). Figure 2 shows the specimen geometry used for conducting tensile tests on HIP welded specimens. The location of the weld interface between the two materials was nearly at the center of the gauge length of the specimens. The specimens were tested in an Instron universal Testing machine for room temperature tensile property evaluation. Selected specimens were examined in SEM for fractographic features and the results were correlated to the surface conditions and tensile properties and microstructures of the specimens.

## Results and Discussion

The SEM study of Nimonic AP-1 powder generally showed the spherical shape with a varying particle size range — Fig. 3. A large number of satellite particles were welded to the surface of large particles — Fig. 3A. At higher magnification, the particles display cellular structure, although dendritic segregation is noticeable in some particles — Fig. 3B. The average grain size, measured by linear intercept method, of the single phase austenitic microstructure of AISI

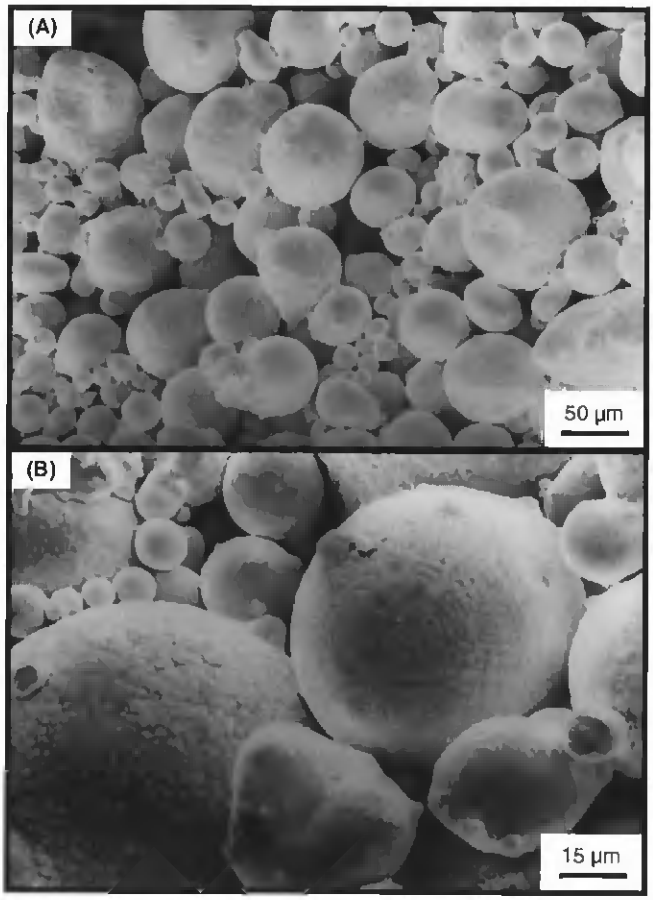


*Fig. 3 — SEM micrographs of argon atomized Nimonic AP-1 powder. A — 200 X; B — 800 X.*

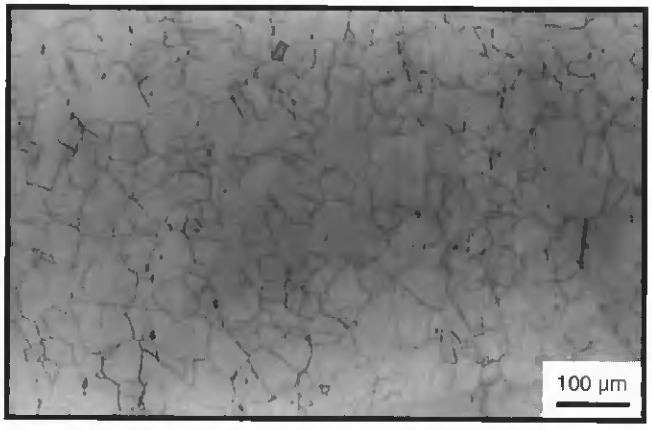


*Fig. 4 — Microstructure of wrought AISI 304 grade stainless steel used for diffusion welding.*

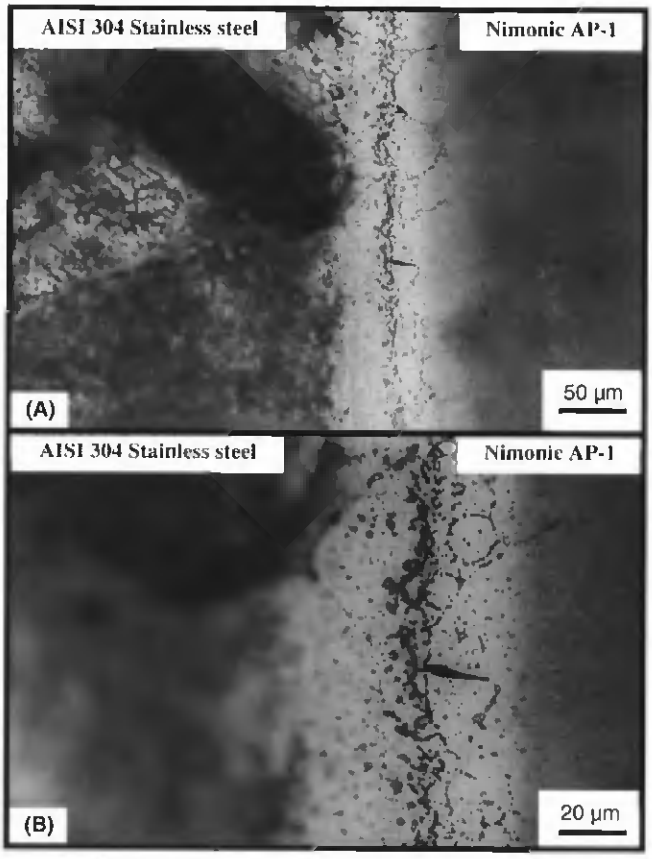


*Fig. 5 — Microstructure of HIP diffusion welded AISI 304 stainless steel with P/M Nimonic AP-1 showing: A — a distinct weld region decorated with dark particles; and B — PPB features noticed in Nimonic AP-1 region near the interface.*

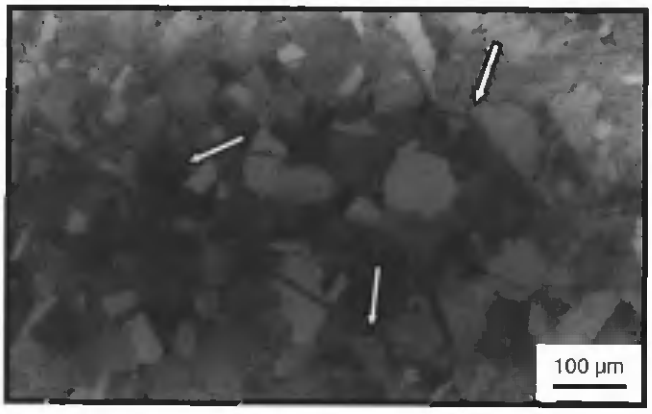


*Fig. 6 — Microstructure of P/M Nimonic AP-1 away from the interface seen in 1200°C-HIP diffusion welded specimen showing PPBs, recrystallized grains and grain growth across the particle boundaries in some areas. Arrows show PPBs.*

304 grade stainless steel material was about 55 μm (Fig. 4).

The representative microstructure of HIP welded materials processed in HIP cycle 1200°C (2192°F)/3 h/147 MPa is shown in Fig. 5. There was no appreciable difference in the microstructure of the specimen HIPed at 1270°C (2318°F)/3 h/121 MPa except for the coarsening of the grains as compared to the lower temperature HIPed material. The weld interlayer was a thin zone ≈ 30–40 μm wide decorated with dark particles at the weld interface. A closer look at the weld interface at higher magnification showed PPB features in Nimonic AP-1 region predominantly near the interlayer — Fig. 5B. The etching characteristics of the two weld materials were markedly different, thus it was not possible to satisfactorily etch the two materials together along with the diffusion welded region.

The characterization of PPB precipitation in Nimonic AP-1 has been done in detail by several investigators (Refs. 13–16) indicating that the PPBs consist of carbides of the type MC, $ZrO_2$, $Al_2O_3$ and borides. The microstructure of P/M Nimonic AP-1 superalloy HIPed at 1200°C (2192°F) away from the weld region revealed PPB networks in many areas (Fig. 6) and reduced tendency of carbide dissolution and redistribution along the grain boundaries. The average grain size of the HIPed Nimonic AP-1 is about 70 μm. The grain size of stainless steel material after HIP treatment was about 160 μm, nearly three times coarser than that of the starting grain size (55 μm). No microporosities or cracks were observed in either HIPed Nimonic AP-1 or at the weld region, indicating sound structure and excellent welding without any defects. The PPB features seen near the weld interlayer are generally undesirable because of their detrimental effect (Refs. 13, 17, 18) on mechanical properties, particularly at elevated temperatures. Also, these particles are known to act as diffusion barriers (Refs. 13, 18) across the particle boundaries and hence, optimization of HIP parameters and/or postconsolidation heat treatment may be required to mitigate these defects and improve the weld properties.

Room temperature tensile tests carried out on HIP welded Nimonic AP-1 and AISI 304 stainless steel specimens for both the HIP cycles led to interesting results. A summary of the tensile test data is given in Table 2. Most of the HIP welded specimens irrespective of surface condition (with one exception) failed in the stainless steel region, indicating that the welded joints are stronger than the stainless steel material. During tensile loading, complete deformation took place in the stainless steel region because of its lower strength as compared to that of Nimonic AP-1 alloy as well as the weld interface. The yield and ultimate strengths of the stainless steel piece in HIP welded specimens are slightly lower than those of the base stainless steel material because of coarsening of grains in AISI 304 stainless steel during diffusion welding at high HIP temperatures. Both the yield and ultimate strengths of Nimonic AP-1 (Ref. 19) at room temperature, as shown in Table 2, are much higher than those values of AISI 304 stainless steel; and hence, tensile results obtained on diffusion welded materials essentially represent properties of AISI 304 stainless steel.

The microstructure of the deformed specimen in the stainless steel region clearly revealed strain induced martensitic transformation — Fig. 7A, which was also confirmed by X-ray diffraction (Fig. 7B). Such transformations have been reported in literature (Refs. 20, 21) for AISI 304L and AISI 304 stainless steels undergoing plastic deformation at room temperature. The volume fraction of martensite is a sigmoidal function of strain and the transformation is very sensitive to temperature in the vicinity of room temperature (Ref. 20). An instability map (Ref. 21) developed recently on the constitutive flow behavior of AISI 304L stainless steel clearly delineated a regime where the enhanced work hardening rate in the strange rate range 0.001–0.01 $s^{-1}$ and at room temperature was due to the formation of martensite. However, the microstructure in the HIPed Nimonic AP-1 region and at the weld interface remained essentially unchanged after tensile testing.

There is a wide gap in ductility values between that of the wrought AISI 304 stainless steel (55%) and the HIP welded

**Table 2 — Room Temperature Tensile Properties of AISI 304 Stainless Steel, HIPed Nimonic AP-1 Superalloy and Diffusion Welded Specimens**

| Materials for Diffusion Welding | Processing Details | Surface Condition | 0.2% Y.S. (MPa) | U.T.S. (MPa) | El. (%) | Remarks |
|---|---|---|---|---|---|---|
| AISI 304 Stainless steel (solid) | wrought | — | 254 | 580 | 55 | — |
| Nimonic AP-1 powder (Ref. 19) | HIPed at 1180°C/3 h 110 MPa | — | 834 | 1285 | 20 | Fully dense. |
| AISI 304 stainless steel + Nimonic AP-1 powder | HIP diffusion welded at 1200°C/ 3 h/ 147 MPa | Acid treated | 276 | 500 | 9 | Fracture in weld. |
| | | Sand blasted | 193 | 257 | 1 | Fracture in weld. |
| | | Smooth finish | 181 | 573 | 15 | *Fracture in SS. |
| | | Rough finish | 237 | 543 | 13 | *Fracture in SS. |
| | HIP diffusion welded at 1270°C/ 3 h/ 121 MPa | Acid treated | 222 | 565 | 17 | *Fracture in SS |
| | | Sand blasted | 265 | 307 | 1 | Fracture in weld. |
| | | Smooth finish | 226 | 565 | 19 | *Fracture in SS. |
| | | Rough finish | 226 | 595 | 16 | *Fracture in SS. |

*All the deformation took place in stainless steel (SS) region.

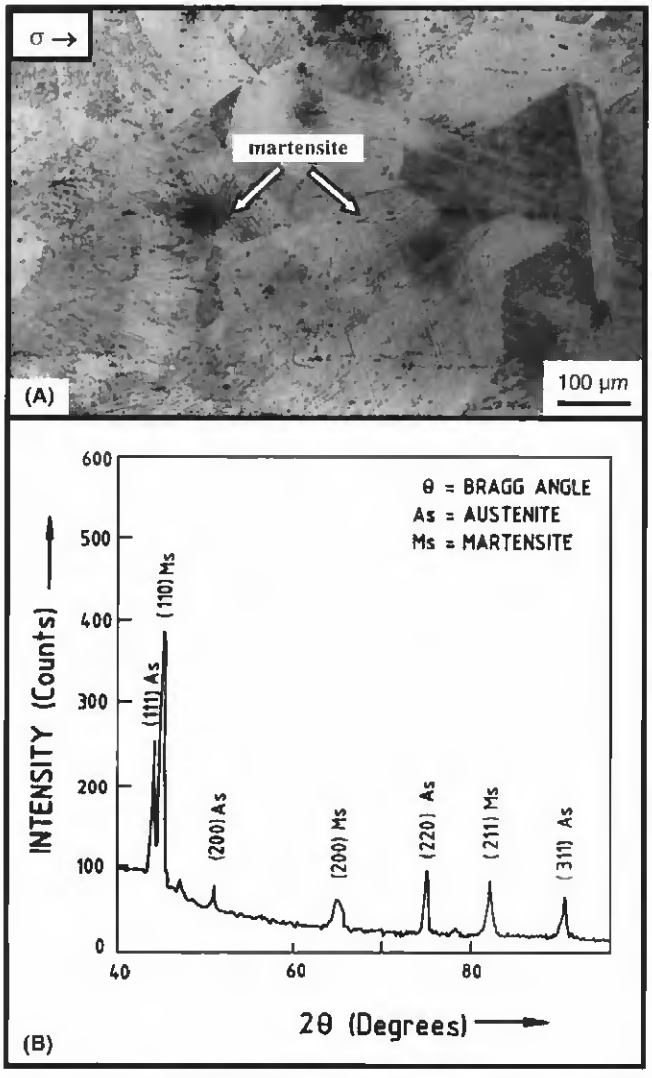


*Fig. 7 — A — Microstructure of RT tensile tested specimen recorded in stainless steel region showing strain induced martensitic transformation. The arrow shows the tensile axis. B — X-ray diffraction pattern showing diffraction peaks for austenite and martensite phases.*

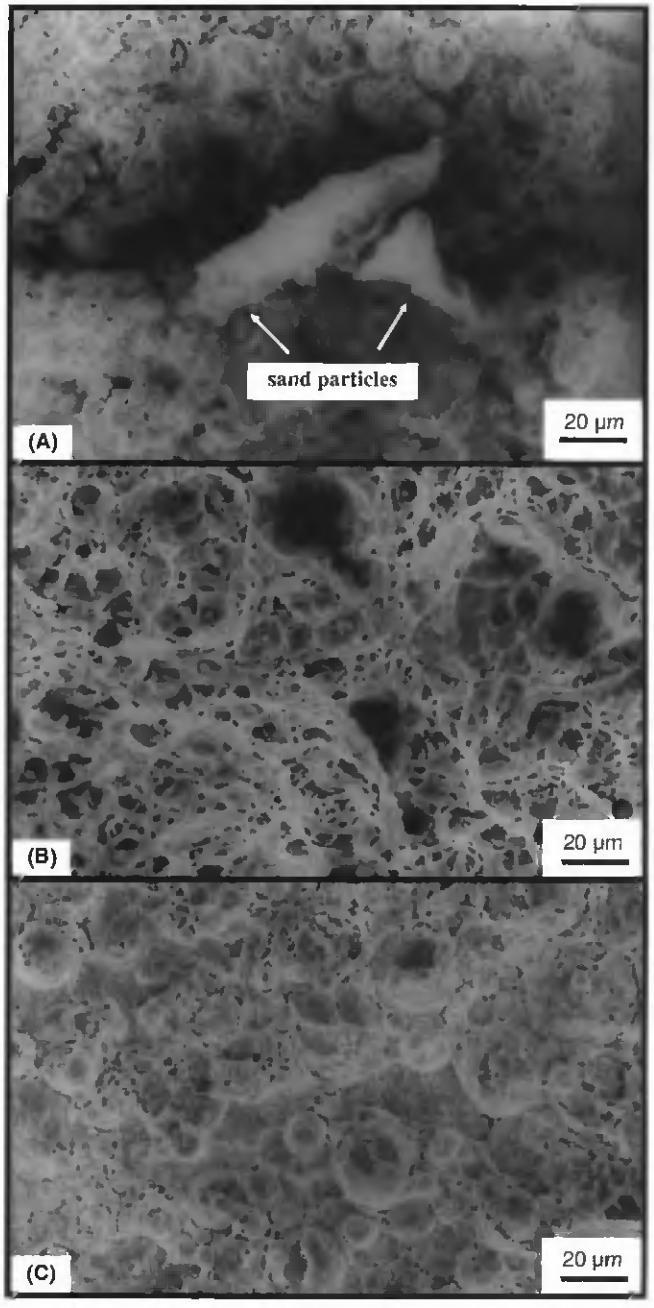


*Fig. 8 — SEM micrographs showing effects of the fracture surface condition on room temperature tensile specimens in HIP diffusion welded AISI 304 stainless steel/ Nimonic AP-1 superalloy powder system. A — Sand blasted surface condition (HIPed at 1270°C); B — Smooth finished surface condition (HIPed at 1200°C); and C — Acid treated surface condition (HIPed at 1200°C).*

materials (13–19%) other than those fractured in the weld region. This is due to the fact that the ductility in the later material has been calculated on the basis of total gauge length comprising both Nimonic AP-1 and stainless steel, the weld interlayer being approximately at the center of the gauge length — Fig. 2. Also, the understanding of the total elongation achieved in austenitic stainless steels is complicated by the strain induced martensitic transformation which, in turn, depends on alloy chemistry, temperature and strain rate (Ref. 20). While those specimens with sand blasted surface condition gave virtually no ductility after HIP welding (1%, Table 2), at both the HIP cycles followed by fracture in the weld region, the 1200°C (2192°F) HIP welded specimen with acid treated surface showed 9% ductility followed by fracture in the weld region, probably due to inadequate HIP processing temperature for this surface condition. These ductility values have not been compared with the ductility of wrought AISI 304 stainless steel as deformation to fracture did not occur in the stainless steel region, unlike other diffusion welded specimens.

A comparison of fractured specimens examined in SEM is shown in Fig. 8. The specimens with sand blasted surface condition clearly revealed the presence of sand particles embedded in the surface (Fig. 8A), which were responsible for crack initiation. While fracture surfaces of other specimens showed ductile failure in the stainless steel region (Fig. 8B), one of the specimens with acid-treated surface condition had failure at the weld region essentially along PPBs (Fig. 8C) indicating that the low temperature HIP diffusion welding at 1200°C (2192°F) led to particle boundary decohesion.

It appears that surface finish in the range of 5–100 µm did not make any appreciable difference in the welding characteristics irrespective of HIP temperature. But the samples having a surface finish of 50 µm showed the presence of sand particles in their room temperature tensile fracture surface (Fig. 8A), because of the use of sand blasting for the preparation of this surface.

The microstructures of samples diffusion welded at 1270°C (2318°F) showed incipient melting in Nimonic AP-1 region (Fig. 9) as compared to that of 1200°C (2192°F) HIP materials — Fig. 6. Also, the fairly large grain growth occurred. This incipient melting did not affect the strength of the weld as failures were in the stainless steel region.

One of the HIP welded specimens was systematically examined for elemental distribution near the weld region in EPMA. The X-ray elemental mapping carried out for different elements qualitatively revealed a clear picture of diffusion across the weld region. Figure 10 shows enrichment of Ti-rich phases along PPBs at interlayer which are mainly carbides/oxycarbides, for a specimen diffusion welded at 1200°C (2192°F)/3 h/147 MPa. A careful study of Cr-map reveals that there is a likelihood of partial depletion of chromium at some regions along PPBs. In all, the map shows fairly uniform distribution of chromium in both materials. While there is evidence of diffusion of Ni, Co and to some extent Al, from Nimonic AP-1 to AISI 304 stainless steel over small distances across the interlayer (≈ 40–50 µm), Fe seems to have diffused in the direction of Nimonic AP-1. The Mn-map reveals a relatively uniform distribution. The Mo-map showed relatively low concentration in Nimonic AP-1 and very small diffusion across the weld region. While the weld properties are likely to be affected because of concentration of Ti-rich carbides at PPBs, the diffusion of major elements such as Ni, Co, Al, Fe, etc., over small distances definitely has a desirable effect on weld characteristics (Ref. 10). Further study in the direction of optimization of HIP parameters, quantitative analysis across the bond region for chemistry of the interface and realization of bimetallic parts is in progress.

## Summary and Conclusions

1) Both the HIP cycles, *i.e.*, 1200°C (2192°F)/3 h/141 MPa and 1270°C (2318°F)/3 h/121 MPa, were found to be capable of producing good diffusion welded joints for wrought AISI 304 stainless steel with Nimonic AP-1 superalloy powder.

2) Surface of wrought AISI 304 stainless steel prepared by sand blasting led to premature failure because of sand particles getting embedded into the surface. Surface preparation by acid pickling is also not desirable. Other surface preparation by mechanical polishing or filing yielded satisfactory results.

3) Weld strengths are controlled by that of stainless steel because of two to three times higher strength of Nimonic AP-1 superalloy.

4) HIP cycle at 1270°C (2318°F) leads to incipient melting in Nimonic AP-1 superalloy, but does not affect the weld strength.

5) The analysis of the interface obtained by hot isostatic pressing at 1200°C (2192°F) showed diffusion of Ni, Co and Al in the direction of stainless steel and diffusion of Fe in the direction of Nimonic AP-1 over few tens of micrometers distances from the interface. Ti-rich PPB particles at the weld interface may have adverse effects on the weld properties, particularly at elevated temperatures and thus, postconsolidation thermomechanical processing may become necessary to mitigate these undesirable features.

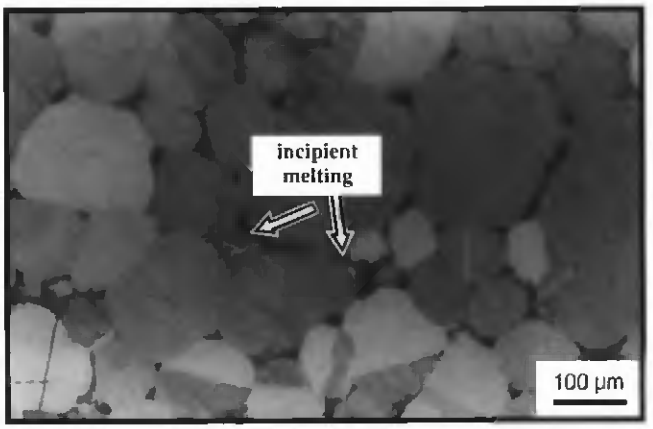


*Fig. 9 — Microstructure showing incipient melting and grain growth in Nimonic AP-1 region of HIP diffusion welded specimens processed at 1270°C/3 h/121 MPa. Arrows show incipient melted regions.*

*Acknowledgments*

The authors would like to thank the Director, DMRL, Hyderabad, for his encouragement and permission to publish this work. Thanks are also extended to Dr. T. L. Prakash, deputy director, DMRL, for providing the HIP facility where the diffusion welding experiments were conducted.

*References*

1. Thamburaj, R., Singer, R. F., and Gessinger, G. H. 1984. *Powder Metallurgy of Superalloys*. Ed. G. H. Gessinger, p. 295, London, Butterworths Monographs in Materials.

2. Nissel, C. 1984. HIP diffusion bonding. *Powder Metallurgy International* 16(3): 113–116.

3. Tsuda, O., Kanamaru, N., Furuta, S., Takigawa, H., and Iwai, K. 1991. PM nickel-base superalloy dual-property disks produced by superplastic forging. *Metal Powder Report* 46(3): 31–35.

4. Iwai, K., Furuta, S., Takigawa, H., Tsuda, O., and Kanamaru, N. 1992. Dual-structure PM nickel-base superalloy turbine disk. *Proc. Intl. Conf. PM Aerospace Materials 1991*. pp. 3.1–3.10. MPR Publishing Services Ltd., Shrewsbury, UK.

5. Jarvenpaa, M. 1988. Consolidation and diffusion bonding of stellite and stainless steel by hot isostatic pressing. *Proc. Intl. Conf. Hot Isostatic Pressing of Materials: Applications and Developments*. pp. 3.1–3.7, Antwerp, Belgium.

6. Romu, K., and Jarvenpaa, M. 1988. Consolidation of stellite and diffusion bonding of stellite and stainless steel by hot isostatic pressing. *Proc. Conf. Hot Isostatic Pressing—Theories and Applications*. Ed. T. Garvare, pp. 269–275, Centek Publishers, Lulea, Sweden.

7. Raisson, G., Rouby, M., and Buekenhout, L. 1988. Diffusion bonding of a low-alloyed steel and nickel-base superalloy (SY 625): Metallurgical Aspect. *Proc. Intl. Conf. Hot Isostatic Pressing of Materials: Applications and Developments*, pp. 3.29–3.31, Antwerp, Belgium.

8. Nisenholz, Z., Mironi, J., and Nir, N. 1986. Diffusion bonding of stainless steel AISI 304L to Ti-6Al-4V alloy. *Proc. 3rd Intl. Conf. Isostatic Pressing ISO 3*. Vol. 1, pp. 33.1–33.10. MPR Publishing Services Ltd., Shrewsbury, UK.

9. Pierronnet, M., and Raisson, G. 1991. The production of clad and bimetal components by the HIP-assisted diffusion bonding of steels and superalloys. *Proc. 4th Intl. Conf. Isostatic Pressing ISO 4*, pp. 30.1–30.14, MPR Publishing Services Ltd., Shrewsbury, UK.

10. Kratt, E. P., Samarov, V. N., Haykin, R. A., and Sobiev, A. S. 1991. Study of HIP rules for processing of bimetallic parts with corrosion resistant coatings. *Powder Metallurgy International* 23(6): 350–353.

11. Kratt, E. P., Sobiev, A. S., Blanter, M. S., Burtsev, A. G., Haykin, R. A., and Samarov, V. N. 1993. Structure and properties of the bonding area in a HIPed steel/superalloy joint. *Powder Metallurgy International* 25(1): 28–30.

12. Somani, M. C., Birla, N. C., and Tekin, A. 1997. Dual properties by hot isostatic diffusion bonding of a nickel base superalloy (under preparation).

13. Thamburaj, R., Wallace, W., Chari, Y. N., and Prakash, T. L. 1984. Influence of processing variables on prior particle boundary precipitation and mechanical behaviour in

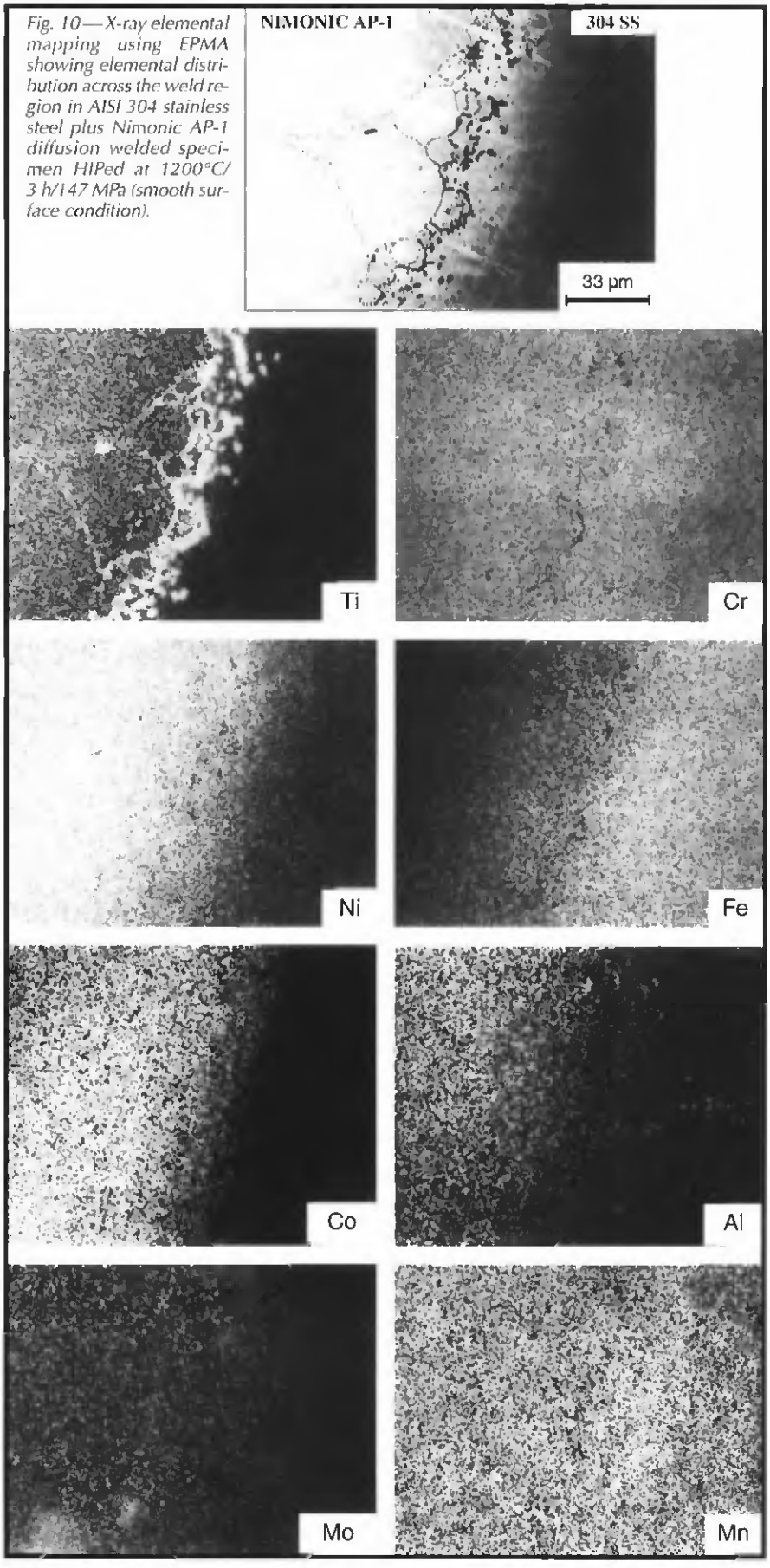


*Fig. 10—X-ray elemental mapping using EPMA showing elemental distribution across the weld region in AISI 304 stainless steel plus Nimonic AP-1 diffusion welded specimen HIPed at 1200°C/3 h/147 MPa (smooth surface condition).*

PM superalloy APK1. *Powder Metallurgy* 27(3): 169–180.

14. Thamburaj, R., Koul, A. K., Wallace, W., and de Malherbe, M. C. 1985. Prior particle boundary precipitation in P/M superalloys. *Modern Developments in Powder Metallurgy*. Eds. E. N. Aque and C. I. Whitman, Vol. 16, p. 635, Metal Powder Industries Federation, Princeton, NJ.

15. Crompton, J. S., and Hertzberg, R. W. 1986. Analysis of second phase particles in a powder metallurgy HIP nickel-base superalloy. *Journal of Materials Science* 21: 3445–3454.

16. Marquez, C., L'Esperance, G., and Koul, A. K. 1989. Prior particle boundary precipitation in Ni-base superalloys. *The International Journal of Powder Metallurgy* 25(4): 301–308.

17. Prakash, T. L., Chari, Y. N., Bhagiradha Rao, E. S., and Thamburaj, R. 1983. Microstructures and mechanical properties of hot isostatically pressed powder metallurgy alloy APK-1. *Metallurgical Transactions A* 14A: 733–743.

18. Somani, M. C., Bhagiradha Rao, E. S., Sarma, G. S., and Sood, R. K. 1986. Characterization and evaluation of hot isostatically pressed low carbon astroloy powder, *Transactions of Indian Institute of Metals* 39(5): 435–444.

19. Somani, M. C., Prakash, T. L., and Bhagiradha Rao, E. S. 1989. *Evaluation of powder processing route for an advanced gas turbine disc superalloy: Part II*. DMRL Technical Report TR 8993, Hyderabad, India, Defence Metallurgical Research Laboratory.

20. Hecker, S. S., Stout, M. G., Staudhammer, K. P., and Smith, J. L. 1982. Effects of strain state and strain rate on deformation — induced transformation in AISI 304 stainless steel: Part I. Magnetic measurements and mechanical behaviour. *Metallurgical Transactions A* 13A: 619–626.

21. Venugopal, S., Mannan, S. L., and Prasad, Y. V. R. K. 1993. Criteria for prediction of flow instabilities and microstructural manifestations during warm working of AISI 304 stainless steel. *Materials Science and Technology*, 9: 1021–1030.